Electronic Supplementary Material (ESI) for Catalysis Science & Technology.

Electronic Supplementary Information

Self-assembly of highly stable and active Co_3O_4/H-TiO_2 bulk heterojunction with high-energy interfacial structures for low temperature CO catalytic oxidation

Zehai Xu,[a] Qingchuan Yin,[a] Xiong Li,[a] Qin Meng,[b] Lusheng Xu,[a]

Boshen Lv [a] and Guoliang Zhang*[a]

TOF measurements

The formula of turnover frequencies for all samples can be calculated as following:

$$\mathrm{TOF}(s^{-1}) = \frac{PV}{RT} \times COvol\% \times conversion\% / \frac{m1 \times m2}{M} / t$$

where P is the pressure (Pa), V is the volume of reactant gases through the reactor every minute (mL), R is the gas constant, and T is the room temperature (K), m1 is mass of total catalyst (g), m2 is mass percent of supported metal and M is the molar mass (g/mol).

Apparent activation energy measurements

The specific reaction rate K can be calculated assuming the ideal gas behaviour as follows:

K (mol g^{-1} s^{-1}) = GHSV (mL h^{-1} g^{-1}) × 1/3600 (h s^{-1}) × 1/1000 (L mL^{-1}) × CO vol.% × conversion% × 1/22.4 (mol L^{-1}) (1)

The specific reaction rate could be expressed by the Arrhenius equation:

$K = A \exp(-E_a/RT)$ (2)

where K is the reaction rate of CO (mol CO g^{-1} s^{-1}), A is the pre-exponential factor (s^{-1}), Ea is the apparent activation energy (kJ mol^{-1}), R is the gas constant, and T is the absolute temperature (K).

Taking the natural log of both sides of the equation (2), we get:

$\ln K = -E_a/T + \ln A$ (3)

By plotting ln K versus 1000/T, the apparent activation energy E_a can be calculated from the slope as shown in Fig. 5.

Table S1. The area percentages of O elemental components calculated from the XPS spectra.

	O 1s			
Samples	O_{Ti-O} (%)	O_{Co-O} (%)	$O_{Ti-O-Co}$ (%)	O_v (%)
C-TiO_2	89.12	\	\	10.88
Co_3O_4/C-TiO_2	58.57	18.89	11.02	11.52
H-TiO_2	88.54	\	\	11.46
Co_3O_4/H-TiO_2	55.26	17.63	12.79	14.32

Table S2. Comparison of TOF and stability with cobalt-based catalysts in literature.

Catalysts	Morphology	TOF(s^{-1}) (120℃)	Time on stream (h)	Ref
Co_3O_4	nanoparticles	7.79×10^{-4}	20	S1
Co_3O_4/ Ni foam	nanoarrays	3.54×10^{-4}	60	S2
Co_3O_4	nanoparticles	9.08×10^{-4}	12	S3
Co_3O_4	nanoparticles	2.27×10^{-3}	24	S4
Co_3O_4/CeO_2	core-shell nanowires	2.47×10^{-3}	\	S5
Co_3O_4	nanosheets	1.91×10^{-3} (100℃)	\	S6
Co_3O_4/SiO_2	nanoparticles	1.32×10^{-3}	\	S7
N-Co_3O_4	nanosheets	8.58×10^{-4}	\	S8
Co_3O_4/CeO_2	nanoparticles	2.70×10^{-3}	\	S9
Co_3O_4/CeO_{2-x}	nanoparticles	3.15×10^{-4}	100	S10
Co_3O_4/CeO_2	nanorods	6.60×10^{-4}	\	S11
Co_3O_4/SiO_2	multi-yolk-double-shell	3.24×10^{-3} (100℃)	28	S12
Co_3O_4/Al_2O_3	nanorods	7.37×10^{-4}	\	S13
Co_3O_4	nanosheets	1.97×10^{-3} (110℃)	6	S14
Co_3O_4/H-TiO_2	cross-section octahedron	3.56×10^{-3}	93	This work
Co_3O_4/C-TiO_2	cross-section octahedron	1.79×10^{-3}	42	
Co_3O_4/P25	nanoparticles	1.28×10^{-3}	21	

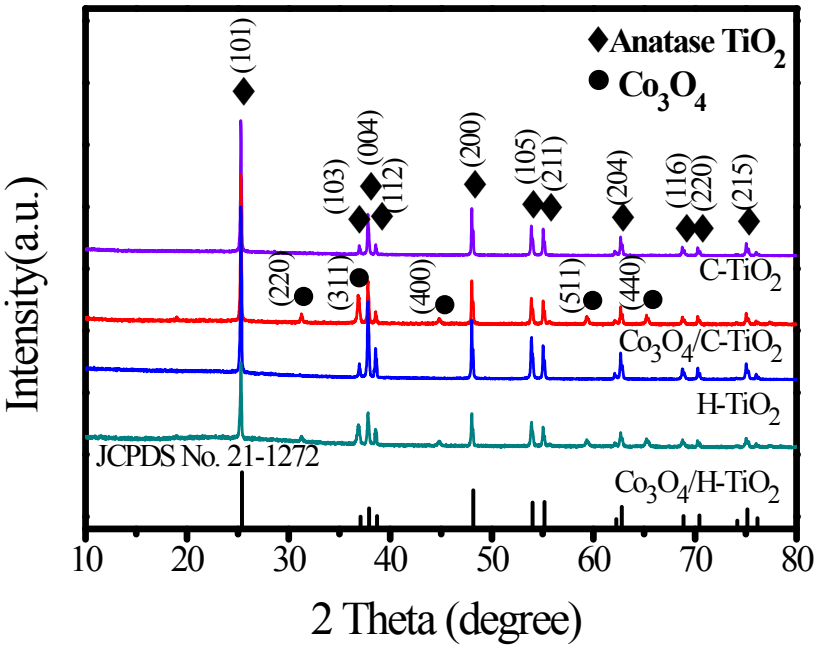

Fig. S1. XRD patterns of C-TiO_2, H-TiO_2, Co_3O_4/C-TiO_2 and Co_3O_4/H-TiO_2. The results demonstrate that preferential growth orientation of H-TiO_2 is [112] direction. After loading Co_3O_4 nanoparticles, some small peaks appeared in the patterns.

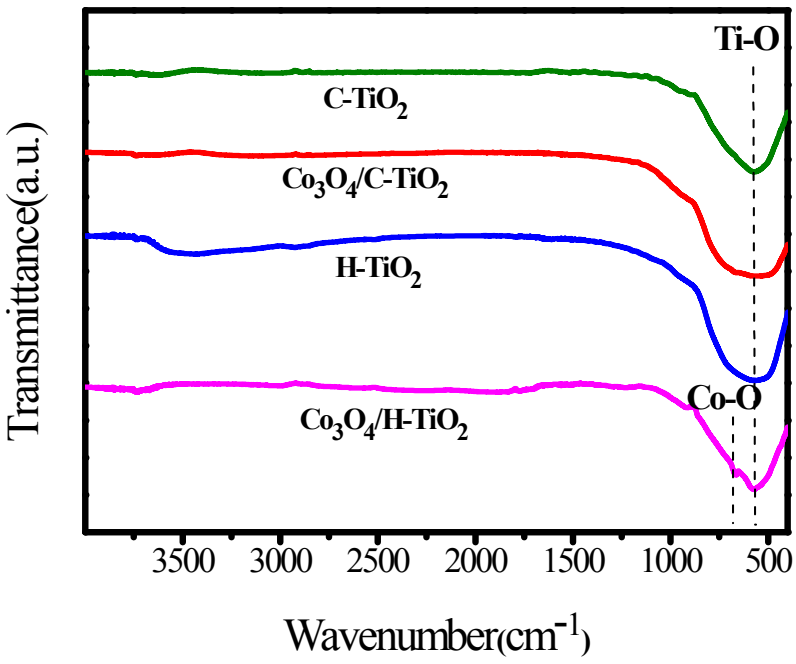

Fig. S2. FTIR spectra of C-TiO_2, H-TiO_2, Co_3O_4/C-TiO_2 and Co_3O_4/H-TiO_2.

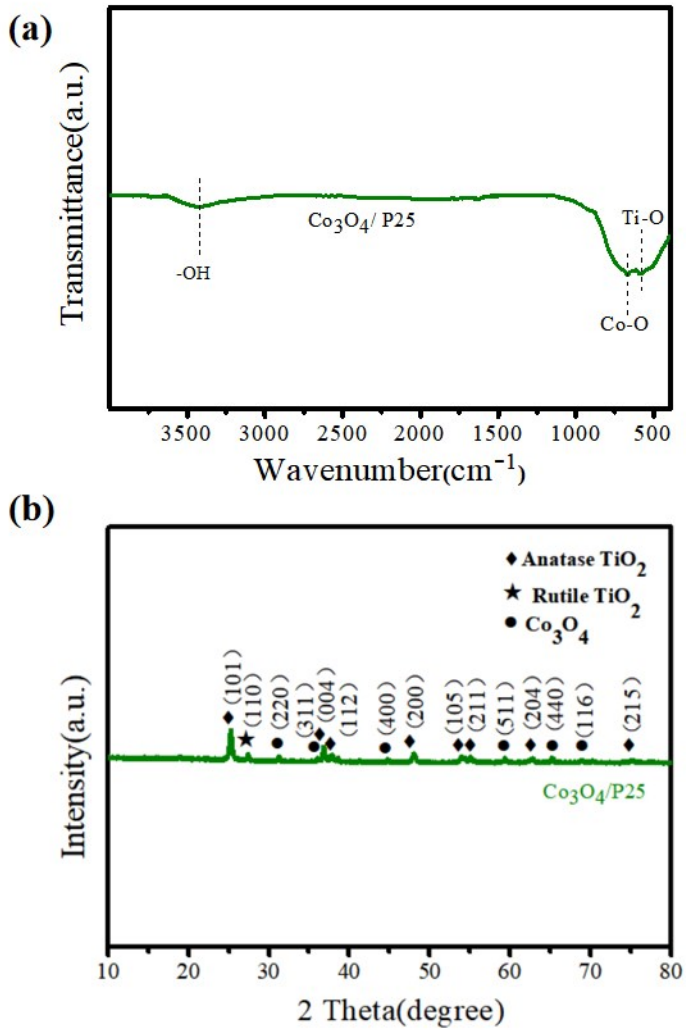

Fig. S3. FTIR spectrum of Co_3O_4/P25 (a) and XRD pattern of Co_3O_4/P25 (b). The generated Co-O bond in FTIR spectrum and new small peaks in XRD pattern demonstrate that Co_3O_4 nanoparticles were successfully loaded on P25 supports.

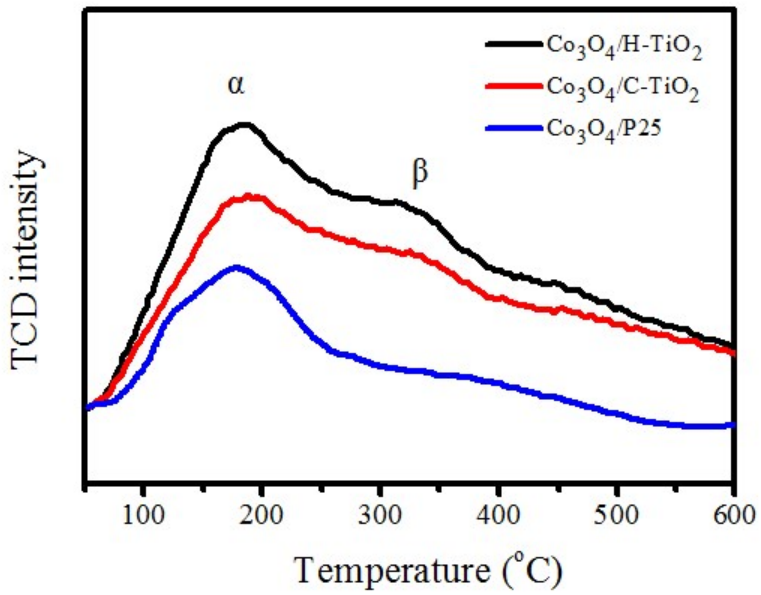

Fig. S4. CO-TPD profiles of different catalysts.

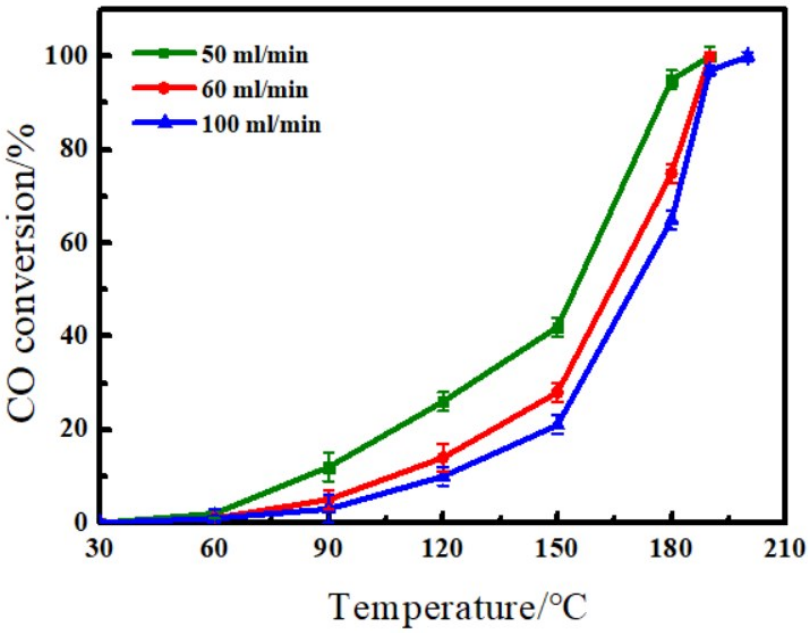

Fig. S5. Conversion rate of catalytic oxidation of CO by Co_3O_4/H-TiO_2 at different flow rates of mixed gas (N_2: 98%, O_2: 1%, CO: 1%).

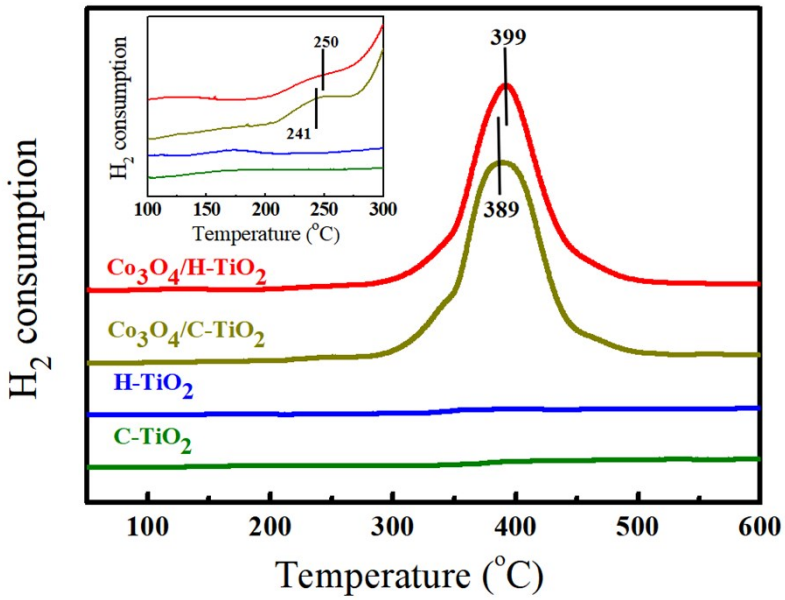

Fig. S6. H_2-TPR diagram of synthesized catalysts.

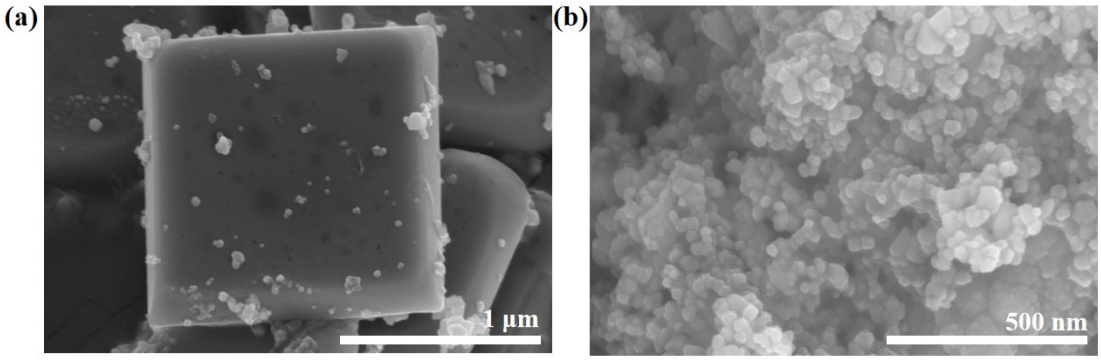

Fig. S7. SEM images of Co_3O_4/C-TiO_2 (a) and Co_3O_4/P25 (b) samples after multiple uses in catalysis.

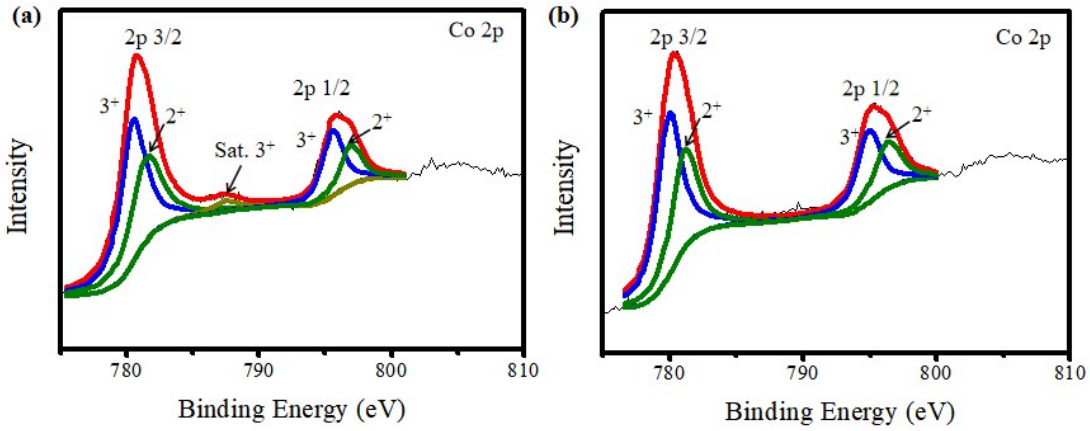

Fig. S8. Co 2p spectra of Co_3O_4/H-TiO_2 (a) and Co_3O_4/C-TiO_2 (b) after CO oxidation reaction.

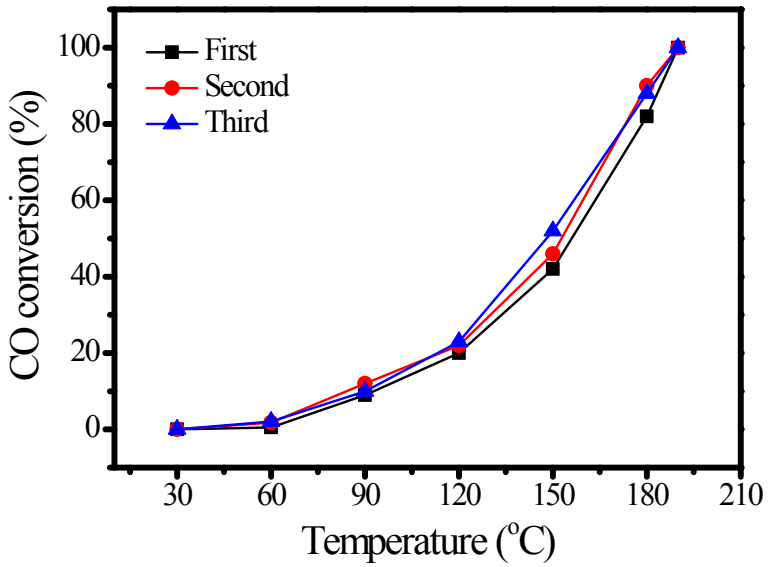

Fig. S9. Reusability of catalysts after subsequent reactions. The catalysts can be recovered to their initial state simply through regenerations up to three cycles.

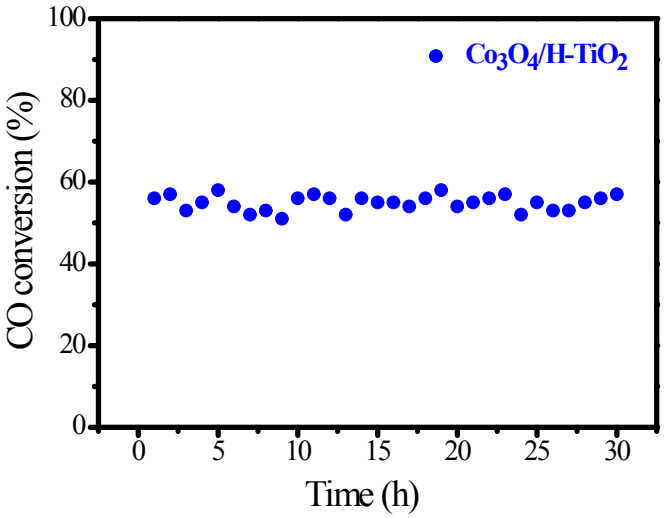

Fig. S10. Long-term stability test of prepared Co_3O_4/H-TiO_2 catalyst under moisture-rich conditions (~2% H_2O) at 180 °C. The Co_3O_4/H-TiO_2 bulk heterojunction can keep attractive activity in the presence of steam for 30 h, revealing high water resistance properties.

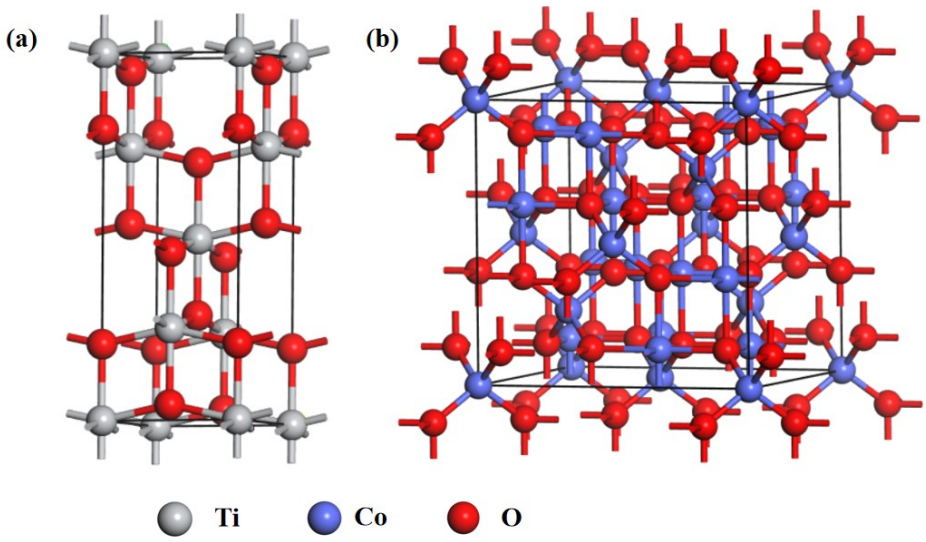

Fig. S11. Physical models of anatase TiO_2 (a) and cubic Co_3O_4 (b). The models of anatase TiO_2 and cubic Co_3O_4 were constructed with parameters derived from JCPDS 21-1272 and JCPDS 42-1467, respectively.

References:

S1. S. J. Deng, X. C. Xiao, X. X. Xing, J. M. Wu, W. Wen, Y. D. Wang, *J. Mol. Catal. A: Chem.*, 2015, **398**, 79-85.

S2. S. P. Mo, S. D. Li, Q. M. Ren, M. Y. Zhang, Y. H. Sun, B. F. Wang, Z. T. Feng, Q. Zhang, Y. F. Chen, D. Q. Ye, *Nanoscale*, 2018, **10**, 7746-7758.

S3. M. H. Li, F. F. Bi, Y. D. Xu, P. P. Hao, K. Xiang, Y. Zhang,S. Y. Chen, J. Guo, X. F. Guo, W. P. Ding, *ACS Catal.* 2019, **9**, 11676-11684.

S4. Z. J. Chen, Y. J. Wang, Q. N. Liang, L. Y. Chen, W. T. Zhan, Y. W. Li, *Sci. China Mater.* 2020, **63**, 267-275.

S5. J. M. Zhen, X. Wang, D. P. Liu, Z. Wang, J. Q. Li, F. Wang, Y. H. Wang, H. J. Zhang, *Nano Res.*, 2015, **8**, 1944-1955.

S6. X. Y. Wang, X. Y. Li, J. C. Mu, S. Y. Fan, X. Chen, L. Wang, Z. F. Yin, M. Tade, S. M. Liu, *ACS Appl. Mater. Inter.*, 2019, **11**, 41988-41999.

S7. N. Yan, Q. W. Chen, F. Wang, Y. Wang, H. Zhong, L. Hua, *J. Mater. Chem. A.*, 1, **2013**, 637-643.

S8. C. C. Yin,Y. A. Liu, Q. N. Xia,S. F. Kang, X. Lib, Y. G. Wang, L. F. Cui, *J. Colloid Interf. Sci*., 2019, **553**, 427-435.

S9. L. Lukashuk, K. Fottinger, E. Kolar, C. Rameshan, D. Teschner, M. Havecker, A. Knop-Gericke, N. Yigit, H. Li, E. McDermott, M. Stoger-Pollach, G. Rupprechter, *J. Catal.*, 2016,344, 1-15.

S10. H. Wang, D. Mao, J. Qi, Q. H. Zhang, X. H. Ma, S. Y. Song, *Adv. Funct. Mater.*, 2019, **29**, 1806588.

S11. J. Q. He, D. Y. Chen, N. J. Li, Q. F. Xu, H. Li, J. H. He, J. M. Lu, *Chemsuschem.*, 2019, **12**,1084-1090.

S12. Y. J. Wang, Z. J. Chen, R. Q. Fang, Y. W. Li, *Chemcatchem.*, 2019, **11**, 772-779.

S13. J. Yang, J. Guo, Y. B. Wang, T. Wang, J. Gu, L. M. Peng, N. H. Xue, Y. Zhu, X. F. Guo, W. P. Ding, *Appl. Surf. Sci.*, 2018, **453**, 330-335.

S14. C. X. Xu, Y. Q. Liu, C. Zhou, L. Wang, H. R. Geng, Y. Ding, *Chemcatchem.*, 2011, **3**, 399-407.